




Impact of the molecular architecture of polycarboxylate superplasticizers on the dispersion of multi-walled carbon nanotubes in aqueous phase

Marco Liebscher^{1,*} , Alex Lange², Christof Schröfl¹, Robert Fuge³, Viktor Mechtcherine¹, Johann Plank², and Albrecht Leonhardt³

¹Institute of Construction Materials, Technische Universität Dresden, 01062 Dresden, Germany

²Chair for Construction Chemistry, Technische Universität München, Lichtenbergstraße 4, 85747 Garching, Germany

³Leibniz-Institut für Festkörper und Werkstofforschung Dresden e.V., IFW, Helmholtzstraße 20, 01069 Dresden, Germany

Received: 9 August 2016

Accepted: 18 October 2016

Published online:

24 October 2016

© Springer Science+Business
Media New York 2016

ABSTRACT

The working mechanism of carbon nanotube (CNT) dispersion by distinct methacrylate ester-based polycarboxylates (PCEs), all of which are highly efficient cement dispersants, was elucidated. Such duplex functionality of the PCE saves introducing an extra surfactant, which might cause severe adverse reactions in cement-based matrices. Eight PCEs exhibiting well-defined architectures were synthesized, characterized by gel permeation chromatography, and their influence on the dispersion capability of CNTs was assessed. The PCEs varied systematically with respect to their backbone length, grafting density, and side-chain length. Using optical microscopy, it was found that at a mass ratio of CNT:PCE = 1:1, pronounced differences manifested themselves in the state of the macro-dispersions, depending on the PCE architecture. However, a clear correlation between PCE structure and dispersing efficiency could not be established. A subsequent study applying equivalent numbers of PCE molecules revealed clear differences in the individual PCEs' dispersibilities. The most efficient PCEs consisted of a long backbone combined with a high side-chain density. Lower side-chain densities as well as short backbones resulted in pronounced reduction in CNT-dispersing ability. Regarding side-chain length, no significant effect was found. Finally, a model for the dispersing mechanism leading to deagglomeration of the CNTs was proposed.

Address correspondence to E-mail: marco.liebscher@tu-dresden.de

Introduction

In the past three decades, carbon nanotubes (CNTs) have been one of the most frequently investigated substances in materials science due to their extraordinary properties, such as high electrical and thermal conductivity as well as mechanical properties [1, 2]. Combined with their tubular geometry and high aspect ratio, they seem to be ideal fillers in preparing multifunctional nanocomposites, including concretes modified with CNTs [3–5]. In numerous applications, the benefits of CNTs can only be exploited if the nanotubes are spread throughout the matrix as individual, unscrambled tubes. However, strong VAN DER WAALS forces between CNTs commonly result in large agglomerates with high mechanical strength [6]. The challenges regarding their effective dispersion have not yet been mastered and continue to be one of the main factors which hinder their broad application in market-relevant fields. In particular, incompatibility between CNTs and the desired base fluid for the dispersion is often a problem. Later on, embedding CNTs in a matrix can as well be thermodynamically unfavorable, for example in the case of cement or polymers. DRESEL and TEIPEL reported better CNT dispersibility in liquids when the surface energies of the polar and dispersive parts of CNTs and of the liquid media were similar [7]. Hence, it is difficult to disperse non-polar CNTs in highly polar media such as water. Still, several approaches have been developed to enhance CNT dispersion in aqueous media, mostly accompanied by ultrasonication [8, 9]. A very promising approach includes the use of surfactants which physically interact with CNTs and water molecules [10, 11]. Meanwhile, numerous surfactants have been developed, which possess a variety of neutral, anionic, cationic, or zwitterionic functionalities or acrylic moieties to enable improved CNT dispersion [8, 12–14]. The surfactant concentration plays a crucial role regarding the dispersion of CNTs [10]. Nevertheless, the usage of such typical CNT-dispersing surfactants did not show a significant improvement of the mechanical properties of cement-based composites, which had been intended by the implementation of CNTs into the matrix [11].

A further approach to tailor the dispersing ability of CNTs is the introduction of functional groups onto CNT surfaces [15]. To achieve compatibility with water, hydroxyl or carboxylic groups are commonly

attached to the outer walls of multi-walled carbon nanotubes (MWCNTs) to enhance their polarity [16]. Also, the incorporation of nitrogen atoms in CNT tubular structure can improve the hydrophilicity of CNT surfaces [17]. However, such modification of the carbon sheets may severely impair their resistance to fragmentation during ultrasonication [18].

Hence, the motivation to the present study was to systematically elucidate the ability of a renowned group of surfactants compatible with cement for its potency to unscramble CNT agglomerates and shed light on the underlying dispersion mechanism. Such duplex functionality of the CNT surfactant, first dispersing the CNTs and later on the mineral fines in the cement-based paste, pares down the number of substances in the system and, consequently, potential incompatibility phenomena among the ingredients. For cement applications, polycarboxylates have been studied for more than 30 years as dispersing agents, widely called superplasticizers or high-range water-reducing admixtures [19]. Recently, polycarboxylate-based comb-type co-polymers have as well been introduced as a potential surfactant for dispersing CNTs in aqueous medium [3–5, 20]. The benefit of using PCEs as a dispersing agent for CNTs is that this kind of molecules is nowadays commonly used for processing concretes and tailored cement-based composites.

Basically, PCEs are comb-shaped polymers possessing a charged backbone and mostly uncharged, but rather hydrophilic side chains [21]. Considerable efforts have been made to explain the working mechanisms of PCEs in cement-based pastes, mortars, and concretes, including hydraulically unreactive inorganic powder suspensions, while considering the ionic loading in the liquid phase. The most agreed-upon outcomes concerning the working mechanisms of PCEs in these highly solids-loaded systems include the following [19, 22–36]:

- adsorption onto the surface of any positively charged inorganic particle present in the suspension by the charged backbone;
- the side chains protruding freely into the liquid;
- a combined dispersive force resulting from both electrostatic repulsion and steric hindrance, the more important part being the steric one;
- the inability of particles to agglomerate;
- the ability to cover freshly evolving surfaces efficiently (i.e., in early hydration products of

- cement, the most important of these being ettringite); and
- significantly reduced losses of both yield stress and plastic viscosity, whereby the specific effect of the PCEs on each of the rheological parameters strongly depends on the polymer composition and architecture.

By selecting these kinds of ionic groups and comonomers constituting the backbone, thus defining the positioning of the ionic groups along it, the backbone's length, the grafting density, and the composition and length of the side chains, enormous variability in molecular design can be achieved to provide optimum performance in specific applications. PCEs have become a crucial component in contemporary cement-based construction materials, in both "high-performance" and "common bulk" applications. Taking this into account, one can be sure that CNT-enhanced, cement-based materials will contain PCEs as well. Hence, utilizing PCEs for pre-dispersing CNTs provides an effective approach for the production of CNT/cement composites. Such pre-dispersion should be studied in plain water. Ionic solutions which mimic cement pore solution should not be utilized here because the PCE/CNT suspension will be added during the mixing processes of mortar or concrete in the same way as any liquid chemical admixture, i.e., as such or together with mixing water. This approach opens a wide range of new potential PCE applications outside the cement and concrete industry.

Although PCEs have already been applied successfully to disperse CNTs, the mechanism of PCEs' action has not yet been clarified. The greatest stumbling block in this effort is often a lack of knowledge of the actual structures of particular PCEs and/or CNTs, attributed to work with commercial samples. Still, some valuable insights have already been published. Collins et al. compared two non-specified PCEs and reported differences in terms of dispersion quality [37]. Zou et al. discussed that their PCE sample had contained active non-polar groups that adsorbed onto the CNT surfaces as well as polar groups which can attach to the cement particles in the aqueous suspension [38]. Kondofersky-Mintova and Plank used a self-synthesized, well-characterized methacrylic acid-co- ω -methoxypoly(ethylene glycol) methacrylate ester (MPEG-MA) to disperse CNTs [39]. Mendoza et al. reported a stable dispersion of

hydroxyl-functionalized CNTs with a commercial superplasticizer [40]. Numerous further publications have been launched, which describe good dispersion qualities of CNTs in water using commercially available superplasticizers [41–56]. Besides CNTs, the dispersion of carbon nanofibers (CNFs) [20, 44, 45, 48, 53, 56–61], graphene nanoplatelets (GnPs) [45, 62–65], graphene oxide (GO) [66], and carbon black [67] through the use of different PCEs has been reported.

However, no systematic study investigating the improvement in the dispersion of CNTs in water and the impact of specific PCE structures has been published, whereby the CNTs themselves had not been characterized thoroughly. Understanding the structure-to-efficiency relation will be an essential step toward developing a model for the working mechanism of CNT dispersion by using PCEs from the viewpoint of interface science and polymer chemistry. The present manuscript focuses on the influence of specific PCE architectures relative to their ability to disperse MWCNTs. For this purpose, different MPEG-based PCEs possessing different backbone lengths, various side-chain lengths, and altering side-chain densities were synthesized, characterized, and investigated with respect to their dispersing efficiency when mixed with CNTs. Dispersion was generally supported by well-defined ultrasonication. Two approaches were followed: the first being the comparison of dispersibility at equivalent mass ratios of CNT to PCE and the second the use of equivalent amounts of PCE molecules. These experiments and considerations of the architectural features of PCEs were used to develop a plausible model with respect to their effect when dispersing CNTs.

Experimental part

PCE design, synthesis, and characterization

All copolymers under investigation are methacrylic acid-co- ω -methoxypoly(ethylene glycol) methacrylate ester (MPEG-MA) PCEs [19]. They consist of a polymethacrylic backbone with poly(ethylene glycol) (PEG) side chains (Fig. 1). Eight PCEs were designed, synthesized, and characterized (Table 1). They were prepared by grafting methoxypolyethylene glycol (obtained from Clariant, Gendorf/Germany) onto polymethacrylic acid (obtained from DOW Chemical,

Figure 1 Chemical composition of the MPEG-based PCE copolymers (*left*) and a schematic drawing of their molecular architecture (*right*).

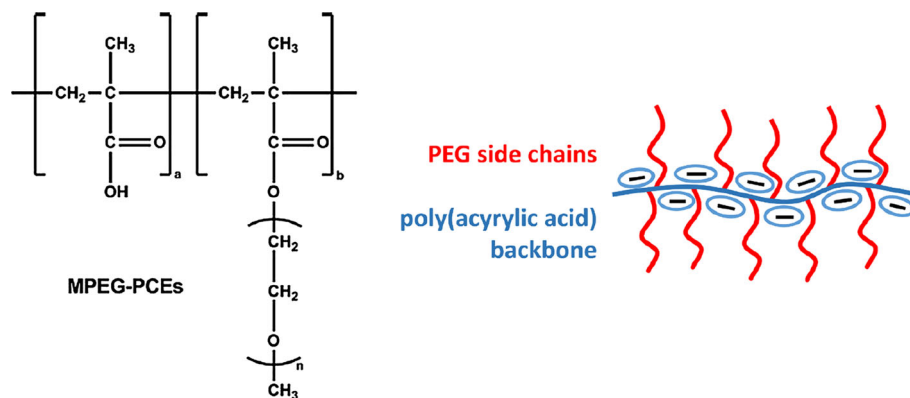


Table 1 Composition of the synthesized PCE samples in respect of their backbone lengths, side-chain lengths, and side-chain densities

PCE sample		Architectural features	
Short backbone	Long backbone	Side-chain length (EO units)	Molar ratio COO ⁻ /side chains, grafting density
17PC6-sb	17PC6-lb	17	6:1, low
17PC1.5-sb	17PC1.5-lb	17	1.5:1, high
45PC6-sb	45PC6-lb	45	6:1, low
45PC1.5-sb	45PC1.5-lb	45	1.5:1, high

Schwalbach/Germany), following a procedure published by Lange and Plank [35].

The first column in Table 1 represents the PCEs of short backbone length, “sb,” which is composed of approximately 83 methacrylic units (based on M_w). In contrast, the second column describes the PCEs exhibiting a long backbone, “lb,” made of about 295 methacrylic units (based on M_w). Additionally, both groups possess two different side-chain lengths as expressed by the numbers “17” and “45” which indicate the number of ethylene glycol units in the laterals. The third parameter in the variation of the PCE structures is their side-chain density. Those with a low side-chain density have one MPEG side chain covalently bonded at every seventh carboxylic moiety of the backbone, the molar ratio of free acid to MPEG ester hence being 6:1 (“PC6”). The second half of the PCE samples possesses a high side-chain density of 1.5:1 (“PC1.5”). All polymer samples were characterized by size exclusion chromatography and static light scattering in an aqueous medium according to the procedures published earlier [35, 68].

Aqueous CNT–PCE dispersions

Multi-walled carbon nanotubes (MWCNTs) of “grade SMW210” were obtained from SWeNT (Norman/OK,

USA). They have a bulk density of 0.07 g/cm³ and a carbon content of 85.92 wt%. According to the supplier, this material represents the primary product as obtained from the synthesis reactor. Hence, it is denominated “as-produced” and the CNTs contain no purposely introduced functional groups.

Deionized water was used to dilute the PCE polymers and to prepare the CNT–PCE aqueous suspensions. Each aqueous dispersion consisted of 17.5 g with a constant CNT content of 0.05 wt%, corresponding to 0.00875 g of absolute CNT mass. In the first part of the study, the CNT-to-PCE mass ratio was fixed at 1:1, based on the content of solids in each PCE solution. Such an approach, which ignores molar masses or other features of the individual PCE samples, is common in practical applications. Subsequently, another study was performed, whereby all samples contained the same number of PCE molecules and at a CNT content of 0.05 wt%. The mass-based study revealed that polymer 17PC1.5-lb had performed best. Hence, the molar amount of this sample, which was considered to be particularly efficient, was calculated. It was taken as standard and from all other PCE samples the same molar amounts were added to the CNT–PCE suspensions.

The mixing was performed under ultrasonication using a Bandelin Sonopuls 3100 instrument

combined with a sonotrode VS70T (Bandelin, Berlin/Germany). A 30 % amplitude and 5 min of mixing time were selected as mixing parameters. These parameters result in an overall energy input of approximately 10 kJ during the entire process and had proven least harmful with respect to CNT length shortening. Reasoning of the selected amplitude, time, and overall energy input has recently been published by Fuge et al. [18]. Ultrasonication was performed in an iced water bath to prevent heating and water evaporation.

CNT characterization

The characterization of the as-received MWCNTs comprised Raman spectroscopy and environmental scanning electron microscopy (ESEM). The Raman spectrum was recorded on a DXR Smart Raman instrument (Thermo Scientific, Waltham, USA), operating at a laser wavelength of 532 nm. The morphology of the CNT agglomerates was assessed by an ESEM Quanta 250 FEG (FEI, Eindhoven/The Netherlands).

Characterization of the aqueous CNT–PCE dispersions

The dispersions were qualitatively characterized with an optical microscope AXIOTECH (Zeiss, Jena/Germany) equipped with a live camera (AxioCam ICc 3, Zeiss, Jena/Germany). Images were recorded in the grey-level mode immediately after mixing the samples. In the optical micrographs, the black areas were taken as an indicator of the effectiveness of the PCEs regarding dispersion because such areas represent the non-dispersed CNT agglomerates. In the sample preparation, two to three drops of the ultrasonicated slurries were

placed between two glass slides using a PASTEUR pipette, the slit having a thickness of about 75 μm , maintained by a spacer. Thus, non-dispersed CNT agglomerates with a native diameter exceeding 75 μm are compressed during the preparation. As a consequence, any CNT agglomerates with sizes larger than 75 μm were not taken into account for quantitative image analysis. However, they appear strikingly large in the micrographs, thus clearly indicating poor deagglomeration.

Results and discussion

Characterization of the PCEs

The results of the gel permeation chromatography (GPC) analysis of the PCEs are summarized in Table 2. From the results obtained, distinct differences between the eight PCEs regarding their architectural features can be recognized.

CNT characterization

The Raman spectrum of the as-received CNTs shown in Fig. 2 exhibits the typical signals for non-purified MWCNTs. A strongly pronounced I_D peak was found at $\sim 1380\text{ cm}^{-1}$, representing a high content of disordered carbon structures including amorphous carbon structures. The I_G peak, which corresponds to the graphitic structure or the state of sp^2 hybridization in the CNTs, can be found at $\sim 1580\text{ cm}^{-1}$ and is significantly lower than the I_D peak. This results in an I_D/I_G ratio of ~ 1.3 . In combination with the pronounced G' peak at $\sim 2690\text{ cm}^{-1}$, the entire spectrum indicates a typical MWCNT structure with a fairly high amount of amorphous carbon and some impurities.

Table 2 Molecular weights of the PCE samples as measured by light scattering

PCE sample	M_w (Da)	M_n (Da)	PDI = M_w/M_n	Architectural features	
				Side chain	Grafting
17PC6-sb	14.800	7.900	1.87	Short	Low
17PC1.5-sb	27.900	13.800	2.02	Short	High
45PC6-sb	27.700	14.900	1.85	Long	Low
45PC1.5-sb	60.700	31.500	1.93	Long	High
17PC6-lb	119.700	28.800	4.16	Short	Low
17PC1.5-lb	201.200	46.400	4.34	Short	High
45PC6-lb	159.800	43.600	3.67	Long	Low
45PC1.5-lb	433.300	105.200	4.12	Long	High

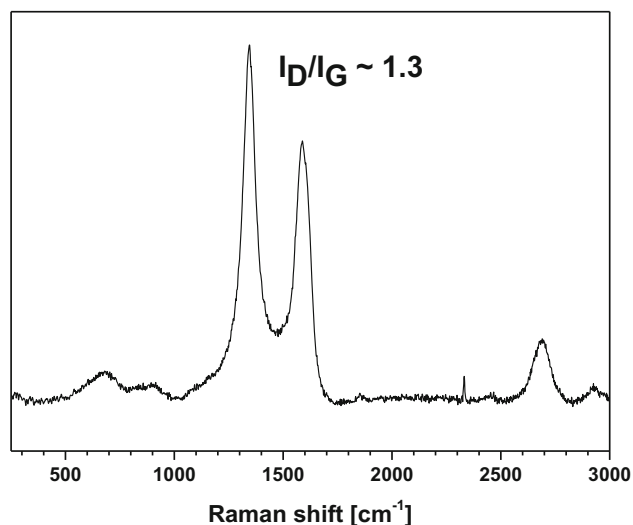


Figure 2 Raman spectrum of the as-received CNTs.

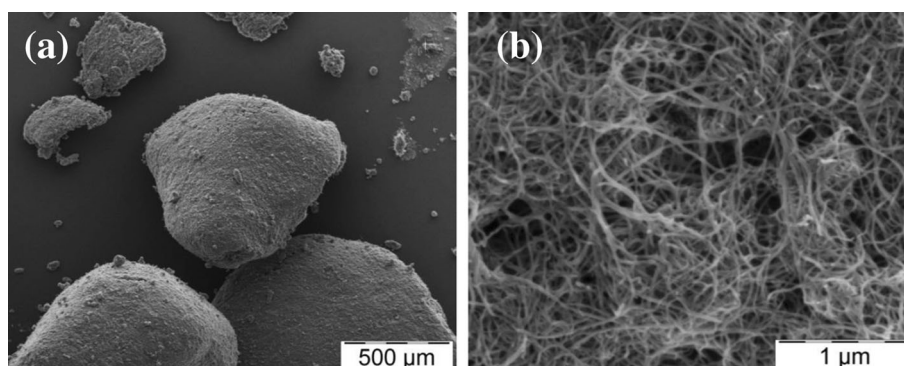
The typical MWCNT structure was also found in the ESEM images of the as-received samples; see Fig. 3a. The CNTs are arranged in large agglomerates having rather spherical shapes with diameters of up to 1 mm. At a higher magnification (Fig. 3b), individual strongly entangled CNTs become visible, which feature diameters of up to 30 nm.

CNT dispersion properties at a PCE:CNT mass ratio of 1:1

Figure 4 shows the optical micrographs of the CNT–PCE samples after ultrasonication. Clear differences in the quality of dispersion are obvious among these samples prepared with a CNT content of 0.05 wt%.

Most of the samples contain numerous non-dispersed agglomerates. This indicates that the input of ultrasonication energy in combination with the dispersive force of the PCE present at 0.05 wt% was insufficient. On the other hand, some specific samples

Figure 3 **a** ESEM images of the MWCNT sample as received showing large agglomerates and **b** detail of a section.



yielded a good macro-dispersion containing no or only very few CNT agglomerates. In particular, the PCEs with long backbones (“lb”) tended to disperse the CNTs better than those with shorter ones (“sb”). Among the PCEs with the long backbone, the ones with shorter side chains produced higher dispersibility, i.e., “17PC” better than “45PC.”

It is here worth to note that a shorter backbone translates into a lower molecular weight compared to PCEs with a longer backbone, provided, of course, that side-chain length and grafting density are alike. Additionally, each “17PC” possesses a lower molar mass than its “45PC” counterpart with the same backbone length and grafting density. Hence, among the eight PCE samples investigated, 45PC1.5-lb contains the fewest molecules per unit of weight (Table 3); however, this PCE sample proved quite good in puncto dispersibility. On the other hand, the PCE sample containing the greatest number of molecules, i.e., 17PC6-sb, produced inferior CNT dispersions.

To summarize, not a single molecular parameter could be found, which appeared to be responsible for the dispersing force of the PCE samples tested. However, large differences in the amounts of PCE molecules present in the suspensions were observed. Thus, it was investigated whether the number of molecules present was the critical parameter for the dispersing effectiveness.

Dispersion effectiveness at equivalent number of PCE molecules

Pronounced differences in CNT dispersion were obtained when using equivalent numbers of PCE molecules as the surfactant (Fig. 5). Similar to the first part of the study, the CNT concentration in the suspension was 0.05 wt%.

Figure 4 Optical micrographs of dispersions prepared with different PCEs after ultrasonication, a CNT:PCE mass ratio of 1:1, and a CNT concentration in the suspension of 0.05 wt%.

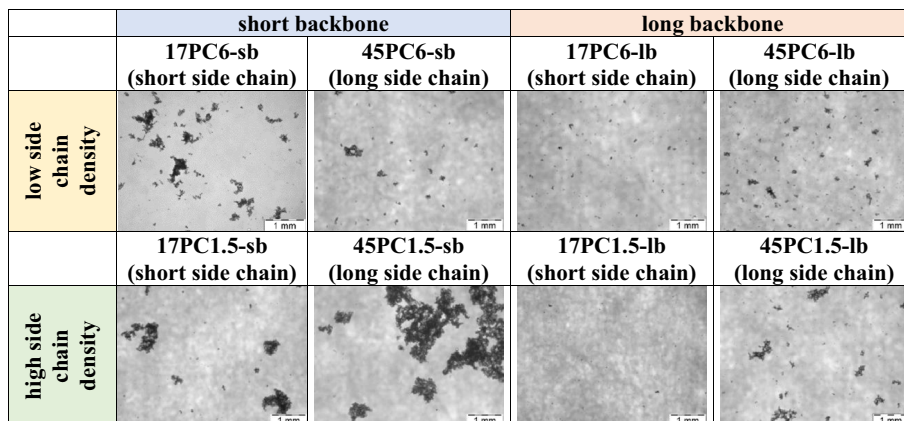
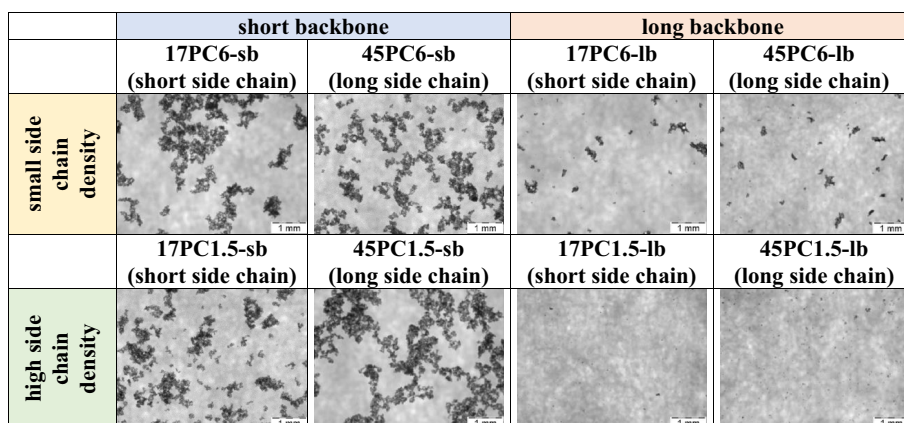


Table 3 Amount n of PCE molecules in each sample at 0.05 wt% PCE dosage

	PCE sample	Mols per sample (10^{-8} mol)	PCE molecules per sample (10^{17})	Side-chain length	Side-chain density
Short backbone	17PC6-sb	111	6.67	Short	Low
	17PC1.5-sb	63	3.82	Short	High
	45PC6-sb	59	3.54	Long	Low
	45PC1.5-sb	28	1.67	Long	High
Long backbone	17PC6-lb	30	1.83	Short	Low
	17PC1.5-lb	19	1.14	Short	High
	45PC6-lb	20	1.21	Long	Low
	45PC1.5-lb	8.3	0.50	Long	High

Figure 5 Optical micrographs of dispersions prepared with the different PCEs after ultrasonication, containing equivalent numbers of PCE molecules per CNT unit mass; CNT concentration in the suspension was 0.05 wt%.



As already mentioned, the samples containing the long-backbone PCEs feature significantly better CNT dispersion than those with the short-backbone PCEs. Among these samples with the short backbone length, neither the side-chain length nor the side-chain density was critical to their performance. Instead, their performance was rather uniform and weak. Contrarily, the dispersing force of the PCEs with long backbones shows differences with respect

to grafting density and side-chain length. A higher side-chain density generally yields better dispersing ability, irrespective of the side-chain length. However, the performance is similar for the same side-chain length or grafting density. Consequently, the two PCE samples exhibiting long backbones and a high side-chain density, i.e., 17PC1.5-lb and 45PC1.5-lb, can produce optimal macro-dispersions which are very nearly free of agglomerates.

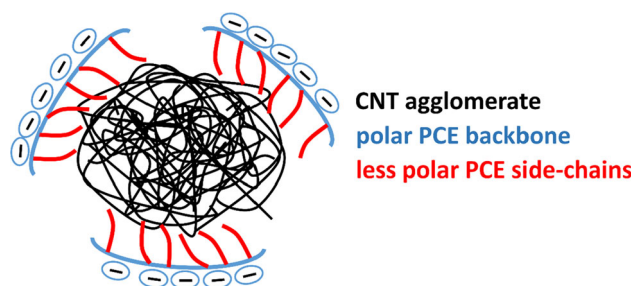


Figure 6 Assumed orientation of MPEG–MA-based PCE comb copolymers along a CNT agglomerate in water.

To sum up, a clear order of efficiency in dispersing the CNTs only exists when equal numbers of PCE molecules are compared. A rather long backbone and a high grafting density are very beneficial, whereas the side-chain length plays no significant role and lower grafting density results in lower efficiency. Furthermore, a shorter main-chain length in the comb-type polymers worsens their dispersing force. Using equal dosages of various PCE products does not allow to constitute a clear structure/efficiency relationship for the PCEs.

Potential dispersing mechanism for CNTs with PCEs

Based on the experimental results as presented, a dispersion mechanism of CNTs using the PCEs under investigation is proposed. Firstly, it must be considered that any PCE copolymer is amphiphilic, which reduces the surface tension of water. This permits better wetting of the pronounced hydrophobic CNT agglomerates. Adding PCE decreases the surface tension of water from 72.8 mN/m for DI water to 60 to 65.5 mN/m, depending on the specific PCE architecture [69]. Furthermore, the two main constituents of PCEs—polymer backbone and graft chains—distinctly affect the surface tension. The polymethacrylic acid part reduces it only very slightly due to the dissociative anionic carboxylic moieties. Ishimuro and Ueberreiter reported a surface tension of more than 72 mN/m at a pH of 7.82 for polymethacrylic acid [70]. Contrary to this, the PEG side chains reduce the surface tension much more, and this effect becomes even more pronounced with increasing molecular weight of the PEG, i.e., with increasing side-chain length [71–73]. Consequently, PCEs with more and longer PEG side chains reduce the surface tension more strongly than those with fewer and shorter ones [69].

Thus, with respect to the surface tension, it is more likely that the PEG part of a PCE attaches to the CNT surface, rather than the backbone does. The more PEG side chains are present in a PCE copolymer, the more intense the interaction between PCE and CNT becomes. Thirdly, longer PEG side chains can be expected to interact even more strongly than the shorter ones. Thus, the polar PCE backbone is most probably oriented toward the water molecules present in the bulk solution, whereas the less polar PEG side chains of the PCE interact with the CNT agglomerates; see Fig. 6.

Considering the different architectural features of the copolymers, the following effects can be concluded with regard to differences in the quality of CNT dispersion. The following considerations are based on the experiments using equal amounts of PCE molecules with respect to CNT.

First, a PCE molecule with a longer backbone possesses a higher specific surface area than the one with a shorter backbone, assuming equal grafting density and side-chain lengths. It is thus more probable for a larger PCE molecule to come in contact with a CNT agglomerate in aqueous suspension than for a smaller one.

Second, at equal mass-based dosage of PCEs with the same grafting density and side-chain length, the same number of PEG dangling bonds is present in the solution, irrespective of backbone length. Hence, when a PCE molecule and a CNT agglomerate come into contact with each other, a PCE with a longer backbone initially brings more PEG side chains into the closest vicinity to, or even into contact with, the CNT agglomerate as compared to a PCE with a shorter backbone at equal grafting density and side-chain length. According to the experimental results, such a PCE has higher CNT-dispersing ability when compared to other PCE architectures, cf. Figure 5. Thus, in this respect the long trunk chain is the most important architectural feature of the PCE.

Third, the higher the grafting density of such PCE copolymers, the more PEG is available for interaction with the CNTs. This results in further improvement of CNT dispersion, as observed for the four PCEs possessing long backbones, e.g., “PC1.5-lb” compared to “PC6-lb.”

Finally, the length of the PEG laterals should be considered. However, according to the optical micrograph in Fig. 5 this molecular parameter

obviously has only a moderate effect on the dispersing force.

Conclusion

This study focused on the effect of various PCE samples on their dispersion efficiency regarding CNTs in an aqueous phase. For the very first time, specific architectural features of the PCEs were taken into account to clarify their impact on the dispersion of CNTs. COLLINS et al. had reported a different state of macro-dispersion using two different commercially available PCE solutions, but had not further focused on mechanistic details [37]. Numerous studies dealt with CNT dispersion by PCE but did not pursue the understanding of distinct efficiencies of individual PCE architectures [38–58]. In general, a PCE product was found to be superior in dispersing CNF when compared to a β -naphthalene sulfonate-based (BNS) superplasticizer sample, the latter species having been reknown as a good cement dispersant for more than 50 years. The explanation was based on the combined electrostatic and steric repulsion evolved by the PCE in contrast to the merely electrostatically acting BNS [20]. Stepping beyond this state of knowledge, the present study provides specific insights to the molecular architectures of PCEs determining their efficiency in dispersing CNTs and the working mechanism behind it.

Eight MPEG-based PCEs were synthesized, each possessing specific architecture with respect to their backbone lengths, side-chain lengths, and side-chain densities. After mixing accompanied by ultrasonication, pronounced differences regarding the quality of CNT dispersion at equal dosages of PCEs under investigation were observed by means of optical microscopy. The mass-based PCE dosages, in the first place, were deliberately chosen because they represent a common approach in practical applications. However, a satisfying structure/effectiveness relationship could not be derived from these experiments.

Using equivalent numbers of PCE molecules (calculated from their M_w) with respect to CNT mass enabled the disclosing of a clear structure/performance relationship. The best dispersion was achieved by PCEs with a long backbone and a high grafting density of PEG laterals.

From these findings, a plausible mechanism was derived in proposing that the PEG side chains interact with CNT agglomerates, while the backbone is toward the water phase [38], similar to the arrangement of surfactant molecules in micelles. Consequently, the PCEs having longer backbone and higher side-chain densities outperform their counterparts which possess short main chains and lower grafting densities.

Interestingly, it was found that side-chain length was far less important when compared to the other two architectural features of the comb copolymers, even despite a strong reduction of the surface tension by increasing PEG molecular weight [71–73].

Our results prove that CNTs are well dispersed by a long-backbone PCE to be incorporated into a cementitious matrix or other water-compatible matrices. Common CNT-dispersing surfactants such as sodium dodecyl sulfate (SDS) or polyoxyethylene (23) lauryl ether (Brij[®] 35), which improved the mechanical properties of cementitious composites only insignificantly [11], can now be replaced by PCEs. These findings contribute strongly to the community of nanotechnology in construction materials, which intensely tries to use PCEs for dispersing carbon-based fillers [3–5].

Looking ahead, the structure/efficiency relation of PCEs should experimentally be extended to further types of CNTs and pooled with recent findings of a most appropriate and gentle ultrasonication procedure [18]. Implementation of the pre-dispersed CNT/PCE suspensions in cement-based construction materials as well as further aquatic, highly loaded inorganic particle suspensions will shed light on the duplex functionality of the PCEs. Effects on hydration, rheological properties, and mechanical performance (bending and compressive strengths) of the cement-based materials will be considered in due course as well. Further characteristic features will be taken into account in application-oriented experiments with other particle suspension, respectively.

Acknowledgements

The authors gratefully acknowledge the financial support of the German Research Foundation (DFG) for its funding of the Projects ME 2938/15-1 and LE 863/19-1.

References

- [1] Krüger A (2010) Carbon nanotubes. In: Carbon materials and nanotechnology. Wiley, Weinheim, pp 123–281
- [2] Thostenson ET, Ren Z, Chou T-W (2001) Advances in the science and technology of carbon nanotubes and their composites: a review. *Compos Sci Technol* 61:1899–1912
- [3] Parveen S, Rana S, Figueiro R (2013) A review on nanomaterial dispersion, microstructure, and mechanical properties of carbon nanotube and nanofiber reinforced cementitious composites. *J Nanomater* 2013:80
- [4] Han B, Sun S, Ding S et al (2015) Review of nanocarbon-engineered multifunctional cementitious composites. *Compos A Appl Sci Manuf* 70:69–81. doi:10.1016/j.compositesa.2014.12.002
- [5] Chuah S, Pan Z, Sanjayan JG et al (2014) Nano reinforced cement and concrete composites and new perspective from graphene oxide. *Constr Build Mater* 73:113–124. doi:10.1016/j.conbuildmat.2014.09.040
- [6] Hilding J, Grulke EA, Zhang ZG, Lockwood F (2003) Dispersion of carbon nanotubes in liquids. *J Dispers Sci Technol* 24:1–41. doi:10.1081/DIS-120017941
- [7] Dresel A, Teipel U (2016) Influence of the wetting behavior and surface energy on the dispersibility of multi-wall carbon nanotubes. *Colloids Surf A* 489:57–66. doi:10.1016/j.colsurfa.2015.10.027
- [8] Kharissova OV, Kharisov BI, Ortiz EGD (2013) Dispersion of carbon nanotubes in water and non-aqueous solvents. *RSC Adv* 3:24812–24852. doi:10.1039/C3ra43852j
- [9] Al-Hamadani YAJ, Chu KH, Son A et al (2015) Stabilization and dispersion of carbon nanomaterials in aqueous solutions: a review. *Sep Purif Technol* 156:861–874. doi:10.1016/j.seppur.2015.11.002
- [10] Vaisman L, Wagner HD, Marom G (2006) The role of surfactants in dispersion of carbon nanotubes. *Adv Colloid Interface Sci* 128:37–46
- [11] Sobolkina A, Mechtcherine V, Khavrus V et al (2012) Dispersion of carbon nanotubes and its influence on the mechanical properties of the cement matrix. *Cem Concr Compos* 34:1104–1113. doi:10.1016/j.cemconcomp.2012.07.008
- [12] Premkumar T, Mezzenga R, Geckeler KE (2012) Carbon nanotubes in the liquid phase: addressing the issue of dispersion. *Small* 8:1299–1313. doi:10.1002/sml.201101786
- [13] Mohamed A, Anas AK, Bakar SA et al (2015) Enhanced dispersion of multiwall carbon nanotubes in natural rubber latex nanocomposites by surfactants bearing phenyl groups. *J Colloid Interface Sci* 455:179–187. doi:10.1016/j.jcis.2015.05.054
- [14] Di Crescenzo A, Di Profio P, Siani G et al (2016) Optimizing the interactions of surfactants with graphitic surfaces and clathrate hydrates. *Langmuir*. doi:10.1021/acs.langmuir.6b01435
- [15] Liebscher M, Gärtner T, Tzounis L et al (2014) Influence of the MWCNT surface functionalization on the thermoelectric properties of melt-mixed polycarbonate composites. *Compos Sci Technol* 101:133–138. doi:10.1016/j.compscitech.2014.07.009
- [16] Osorio AG, Silveira ICL, Bueno VL, Bergmann CP (2008) H₂SO₄/HNO₃/HCl—functionalization and its effect on dispersion of carbon nanotubes in aqueous media. *Appl Surf Sci* 255:2485–2489. doi:10.1016/j.apsusc.2008.07.144
- [17] Sobolkina A, Mechtcherine V, Bellmann C et al (2014) Surface properties of CNTs and their interaction with silica. *J Colloid Interface Sci* 413:43–53. doi:10.1016/j.jcis.2013.09.033
- [18] Fuge R, Liebscher M, Schröfl C et al (2016) Fragmentation characteristics of undoped and nitrogen-doped multiwalled carbon nanotubes in aqueous dispersion in dependence on the ultrasonication parameters. *Diam Relat Mater* 66:126–134. doi:10.1016/j.diamond.2016.03.026
- [19] Plank J, Sakai E, Miao CW et al (2015) Chemical admixtures—chemistry, applications and their impact on concrete microstructure and durability. *Cem Concr Res A* 78:81–99. doi:10.1016/j.cemconres.2015.05.016
- [20] Stephens C, Brown L, Sanchez F (2016) Quantification of the re-agglomeration of carbon nanofiber aqueous dispersion in cement pastes and effect on the early age flexural response. *Carbon*. doi:10.1016/j.carbon.2016.05.076
- [21] Gay C, Raphaël E (2001) Comb-like polymers inside nanoscale pores. *Adv Colloid Interface Sci* 94:229–236. doi:10.1016/S0001-8686(01)00062-8
- [22] Monosi S, Troli R, Coppola L, Collepardi M (1996) Water reducers for the high alumina cement-silica fume system. *Mater Struct* 29:639–644. doi:10.1007/BF02485972
- [23] Uchikawa H, Hanehara S, Sawaki D (1997) The role of steric repulsive force in the dispersion of cement particles in fresh paste prepared with organic admixture. *Cem Concr Res* 27:37–50. doi:10.1016/S0008-8846(96)00207-4
- [24] Yamada K, Takahashi T, Hanehara S, Matsuhisa M (2000) Effects of the chemical structure on the properties of polycarboxylate-type superplasticizer. *Cem Concr Res* 30:197–207. doi:10.1016/S0008-8846(99)00230-6
- [25] Yamada K, Ogawa S, Hanehara S (2001) Controlling of the adsorption and dispersing force of polycarboxylate-type superplasticizer by sulfate ion concentration in aqueous phase. *Cem Concr Res* 31:375–383. doi:10.1016/S0008-8846(00)00503-2

- [26] Sakai E, Yamada K, Ohta A (2003) Molecular structure and dispersion-adsorption mechanisms of comb-type superplasticizers used in Japan. *J Adv Concr Technol* 1:16–25. doi:[10.3151/jact.1.16](https://doi.org/10.3151/jact.1.16)
- [27] Puertas F, Santos H, Palacios M, Martínez-Ramírez S (2005) Polycarboxylate superplasticiser admixtures: effect on hydration, microstructure and rheological behaviour in cement pastes. *Adv Cem Res* 17:77–89
- [28] Sakai E, Ishida A, Ohta A (2006) New trends in the development of chemical admixtures in Japan. *J Adv Concr Technol* 4:211–223. doi:[10.3151/jact.4.211](https://doi.org/10.3151/jact.4.211)
- [29] Plank J, Chatziagorastou P, Hirsch C (2007) New model describing distribution of adsorbed superplasticizer on the surface of hydrating cement grain. Jianzhu Cailiao Xuebao (*J Build Mater*) 10:7–13
- [30] Schröfl C, Gruber M, Plank J (2012) Preferential adsorption of polycarboxylate superplasticizers on cement and silica fume in ultra-high performance concrete (UHPC). *Cem Concr Res* 42:1401–1408. doi:[10.1016/j.cemconres.2012.08.013](https://doi.org/10.1016/j.cemconres.2012.08.013)
- [31] Alonso MM, Palacios M, Puertas F (2013) Compatibility between polycarboxylate-based admixtures and blended-cement pastes. *Cem Concr Compos* 35:151–162. doi:[10.1016/j.cemconcomp.2012.08.020](https://doi.org/10.1016/j.cemconcomp.2012.08.020)
- [32] Habbaba A, Lange A, Plank J (2013) Synthesis and performance of a modified polycarboxylate dispersant for concrete possessing enhanced cement compatibility. *J Appl Polym Sci* 129:346–353. doi:[10.1002/app.38742](https://doi.org/10.1002/app.38742)
- [33] Marchon D, Sulser U, Eberhardt A, Flatt RJ (2013) Molecular design of comb-shaped polycarboxylate dispersants for environmentally friendly concrete. *Soft Matter* 9:10719–10728. doi:[10.1039/C3SM51030A](https://doi.org/10.1039/C3SM51030A)
- [34] Kong F, Pan L, Wang C et al (2016) Effects of polycarboxylate superplasticizers with different molecular structure on the hydration behavior of cement paste. *Constr Build Mater* 105:545–553. doi:[10.1016/j.conbuildmat.2015.12.178](https://doi.org/10.1016/j.conbuildmat.2015.12.178)
- [35] Lange A, Plank J (2015) Optimization of comb-shaped polycarboxylate cement dispersants to achieve fast-flowing mortar and concrete. *J Appl Polym Sci*. doi:[10.1002/app.42529](https://doi.org/10.1002/app.42529)
- [36] Lange A, Hirata T, Plank J (2014) Influence of the HLB value of polycarboxylate superplasticizers on the flow behavior of mortar and concrete. *Cem Concr Res* 60:45–50. doi:[10.1016/j.cemconres.2014.02.011](https://doi.org/10.1016/j.cemconres.2014.02.011)
- [37] Collins F, Lambert J, Duan WH (2012) The influences of admixtures on the dispersion, workability, and strength of carbon nanotube–OPC paste mixtures. *Cem Concr Compos* 34:201–207. doi:[10.1016/j.cemconcomp.2011.09.013](https://doi.org/10.1016/j.cemconcomp.2011.09.013)
- [38] Zou B, Chen SJ, Korayem AH et al (2015) Effect of ultrasonication energy on engineering properties of carbon nanotube reinforced cement pastes. *Carbon* 85:212–220. doi:[10.1016/j.carbon.2014.12.094](https://doi.org/10.1016/j.carbon.2014.12.094)
- [39] Kondofersky-Mintova I, Plank J (2012) Fundamental Interactions between multi-walled carbon nanotubes (MWCNT), Ca²⁺ and polycarboxylate superplasticizers in cementitious systems. In: Malhotra VM (ed) 10th international conference on superplasticizers and other chemical admixtures in concrete, SP-288-29. Farmington Hills (MI/USA), pp 423–434
- [40] Mendoza O, Sierra G, Tobón JI (2013) Influence of super plasticizer and Ca(OH)₂ on the stability of functionalized multi-walled carbon nanotubes dispersions for cement composites applications. *Constr Build Mater* 47:771–778. doi:[10.1016/j.conbuildmat.2013.05.100](https://doi.org/10.1016/j.conbuildmat.2013.05.100)
- [41] Chen SJ, Wang W, Sagoe-Crentsil K et al (2016) Distribution of carbon nanotubes in fresh ordinary Portland cement pastes: understanding from a two-phase perspective. *RSC Adv* 6:5745–5753. doi:[10.1039/C5RA13511G](https://doi.org/10.1039/C5RA13511G)
- [42] Khater HM, Abd el Gawaad HA (2016) Characterization of alkali activated geopolymer mortar doped with MWCNT 102. *Constr Build Mater* 102:329–337. doi:[10.1016/j.conbuildmat.2015.10.121](https://doi.org/10.1016/j.conbuildmat.2015.10.121)
- [43] Shah SP, Konsta-Gdoutos MS, Metaxa ZS (2011) Advanced cement based nanocomposites. In: Kounadis A, Gdoutos E (eds) Recent advances in mechanics. Springer, Netherlands, pp 313–327
- [44] Han B, Zhang K, Yu X et al (2011) Fabrication of piezoresistive CNT/CNF cementitious composites with superplasticizer as dispersant. *J Mater Civ Eng* 24:658–665
- [45] Al-Dahawi A, Öztürk O, Emami F et al (2016) Effect of mixing methods on the electrical properties of cementitious composites incorporating different carbon-based materials. *Constr Build Mater* 104:160–168. doi:[10.1016/j.conbuildmat.2015.12.072](https://doi.org/10.1016/j.conbuildmat.2015.12.072)
- [46] Wille K, Loh K (2010) Nanoengineering ultra-high-performance concrete with multiwalled carbon nanotubes. *Transp Res Record* 2142:119–126. doi:[10.3141/2142-18](https://doi.org/10.3141/2142-18)
- [47] Amin MS, El-Gamal SMA, Hashem FS (2015) Fire resistance and mechanical properties of carbon nanotubes—clay bricks wastes (Homra) composites cement. *Constr Build Mater* 98:237–249. doi:[10.1016/j.conbuildmat.2015.08.074](https://doi.org/10.1016/j.conbuildmat.2015.08.074)
- [48] Konsta-Gdoutos MS, Aza CA (2014) Self sensing carbon nanotube (CNT) and nanofiber (CNF) cementitious composites for real time damage assessment in smart structures. *Cem Concr Compos* 53:162–169. doi:[10.1016/j.cemconcomp.2014.07.003](https://doi.org/10.1016/j.cemconcomp.2014.07.003)
- [49] Correia AAS, Casaleiro PDF, Rasteiro MGBV (2015) Applying multiwall carbon nanotubes for soil stabilization. *Procedia Eng* 102:1766–1775. doi:[10.1016/j.proeng.2015.01.313](https://doi.org/10.1016/j.proeng.2015.01.313)

- [50] Yazdanbakhsh A, Grasley Z, Tyson B, Abu Al-Rub RK (2010) Distribution of carbon nanofibers and nanotubes in cementitious composites. *Transp Res Record* 2142:89–95
- [51] Fakhim B, Hassani A, Rashidi A, Ghodousi P (2015) Preparation and microstructural properties study on cement composites reinforced with multi-walled carbon nanotubes. *J Compos Mater* 49:85–98. doi:[10.1177/0021998313514873](https://doi.org/10.1177/0021998313514873)
- [52] Manzur T, Yazdani N (2014) Optimum mix ratio for carbon nanotubes in cement mortar. *KSCE J Civ Eng* 19:1405–1412. doi:[10.1007/s12205-014-0721-x](https://doi.org/10.1007/s12205-014-0721-x)
- [53] Yazdanbakhsh A, Grasley ZC, Tyson B, Al-Rub RKA (2009) Carbon nano filaments in cementitious materials: some issues on dispersion and interfacial bond. *Special Publ* 267:21–34
- [54] Manzur T, Yazdani N, Emon MAB (2016) Potential of carbon nanotube reinforced cement composites as concrete repair material. *J Nanomater* 2016:e1421959. doi:[10.1155/2016/1421959](https://doi.org/10.1155/2016/1421959)
- [55] Jang S-H, Kawashima S, Yin H (2016) Influence of carbon nanotube clustering on mechanical and electrical properties of cement pastes. *Materials* 9:220. doi:[10.3390/ma9040220](https://doi.org/10.3390/ma9040220)
- [56] Blandine F, Habermehi-Cwirzen K, Cwirzen A (2016) Contribution of CNTs/CNFs morphology to reduction of autogenous shrinkage of Portland cement paste. *Front Struct Civ Eng* 1–12. doi:[10.1007/s11709-016-0331-4](https://doi.org/10.1007/s11709-016-0331-4)
- [57] Tyson BM, Abu Al-Rub RK, Yazdanbakhsh A, Grasley Z (2011) Carbon nanotubes and carbon nanofibers for enhancing the mechanical properties of nanocomposite cementitious materials. *J Mater Civ Eng* 23:1028–1035
- [58] Abu Al-Rub RK, Tyson BM, Yazdanbakhsh A, Grasley Z (2012) Mechanical properties of nanocomposite cement incorporating surface-treated and untreated carbon nanotubes and carbon nanofibers. *J Nanomech Micromech* 2:1–6. doi:[10.1061/\(ASCE\)NM.2153-5477.0000041](https://doi.org/10.1061/(ASCE)NM.2153-5477.0000041)
- [59] Yazdanbakhsh A, Chu C (2015) The effect of carbon nanofibers on the strength of concrete with natural and recycled aggregates. In: Sobolev K, Shah SP (eds) *Nanotechnology in construction*. Springer, New York, pp 277–283
- [60] Lestari Y, Bahri S, Sugiarti E, et al (2013) Effect of different dispersants in compressive strength of carbon fiber cementitious composites. In: *AIP Conference Proceedings*. AIP Publishing, Melville, pp 67–69
- [61] Gay C, Sanchez F (2010) Performance of carbon nanofiber-cement composites with a high-range water reducer. *Transp Res Record* 2142:109–113
- [62] Du H, Pang SD (2015) Enhancement of barrier properties of cement mortar with graphene nanoplatelet. *Cem Concr Res* 76:10–19. doi:[10.1016/j.cemconres.2015.05.007](https://doi.org/10.1016/j.cemconres.2015.05.007)
- [63] Wotring E, Mondal P, Marsh C (2015) Characterizing the dispersion of graphene nanoplatelets in water with water reducing admixture. In: Sobolev K, Shah SP (eds) *Nanotechnology in construction*. Springer, New York, pp 141–148
- [64] Metaxa ZS (2015) Polycarboxylate based superplasticizers as dispersant agents for xGnPs reinforcing cement based materials. *J Eng Sci Technol Rev* 8:1–5
- [65] Du H, Gao HJ, Pang SD (2016) Improvement in concrete resistance against water and chloride ingress by adding graphene nanoplatelet. *Cem Concr Res* 83:114–123. doi:[10.1016/j.cemconres.2016.02.005](https://doi.org/10.1016/j.cemconres.2016.02.005)
- [66] Zhao L, Guo X, Ge C et al (2016) Investigation of the effectiveness of PC@GO on the reinforcement for cement composites. *Constr Build Mater* 113:470–478. doi:[10.1016/j.conbuildmat.2016.03.090](https://doi.org/10.1016/j.conbuildmat.2016.03.090)
- [67] Sharma S, Kothiyal NC (2015) Synergistic effect of zero-dimensional spherical carbon nanoparticles and one-dimensional carbon nanotubes on properties of cement-based ceramic matrix: microstructural perspectives and crystallization investigations. *Compos Interfaces* 22:899–921. doi:[10.1080/09276440.2015.1076281](https://doi.org/10.1080/09276440.2015.1076281)
- [68] Laguna MTR, Medrano R, Plana MP, Tarazona MP (2001) Polymer characterization by size-exclusion chromatography with multiple detection. *J Chromatogr A* 919:13–19. doi:[10.1016/S0021-9673\(01\)00802-0](https://doi.org/10.1016/S0021-9673(01)00802-0)
- [69] Wieneke B (2010) *Neue Ansätze zum Verständnis des Wirkmechanismus von Schwindreduzierern in zementären Systemen*. Verlag Dr. Hut
- [70] Ishimuro PDY, Ueberreiter PDK (1980) The surface tension of poly(acrylic acid) in aqueous solution. *Colloid Polym Sci* 258:928–931. doi:[10.1007/BF01584922](https://doi.org/10.1007/BF01584922)
- [71] Winterhalter M, Bürner H, Marzinka S et al (1995) Interaction of poly(ethylene-glycols) with air-water interfaces and lipid monolayers: investigations on surface pressure and surface potential. *Biophys J* 69:1372–1381
- [72] Nakanishi K, Matsumoto T, Hayatsu M (1971) Surface tension of aqueous solutions of some glycols. *J Chem Eng Data* 16:44–45. doi:[10.1021/je60048a010](https://doi.org/10.1021/je60048a010)
- [73] Wang P, Kosinski JJ, Anderko A et al (2013) Ethylene glycol and its mixtures with water and electrolytes: thermodynamic and transport properties. *Ind Eng Chem Res* 52:15968–15987. doi:[10.1021/ie4019353](https://doi.org/10.1021/ie4019353)